ACS Catalysis

Research Article

pubs.acs.org/acscatalysis

Sustainable and Near Ambient DeNO$_x$ Under Lean Burn Conditions: A Revisit to NO Reduction on Virgin and Modified Pd(111) Surfaces

Kanak Roy,[†] Ruchi Jain,[†] and Chinnakonda S. Gopinath*[,†,‡]

[†]Catalysis Division, National Chemical Laboratory, Dr. Homi Bhabha Road, Pune 411 008, India

[‡]Center of Excellence on Surface Science, National Chemical Laboratory, Dr. Homi Bhabha Road, Pune 411 008, India

Supporting Information

ABSTRACT: Catalytic conversion of NO in the presence of H_2 and O_2 has been studied on Pd(111) surfaces, by using a molecular beam instrument with mass spectrometry detection, as a function of temperature and reactants composition. N_2 and H_2O are the major products observed, along with NH_3 and N_2O minor products under all conditions studied. Particular attention has been paid to the influence of O_2 addition toward NO dissociation. Although O_2-rich compositions were found to inhibit the deNO$_x$ activity of the Pd catalyst, some enhancement in NO reduction to N_2 was also observed up to a certain O_2 content. The reason for this behavior was determined to be the effective consumption of the H_2 in the mixture by the added O_2 and O atoms from NO dissociation. NO was proven to compete favorably against O_2 for the consumption of H_2, especially ≤550 K, to produce N_2 and H_2O. Compared with other elementary reaction steps, a slow decay observed with the 2H + O → H_2O step under SS beam oscillation conditions demonstrates its contribution to the rate-limiting nature of the overall reaction. Pd(111) surfaces modified with O atoms in the subsurface (Md-Pd(111)) induces steady-state NO reduction at near-ambient temperatures (325 K) and opens up a possibility to achieve room temperature emission control. A 50% increase in the reaction rates was observed at the reaction maximum on Md-Pd(111), as compared with virgin surfaces. Oxygen adsorption is severely limited below 400 K, and effective NO + H_2 reaction occurs on Md-Pd(111) surfaces. Valence band photoemission with a UV light source (He I) under different oxygen pressures with APPES clearly identified the characteristics of the Md-Pd(111) surfaces and PdO. The electron-deficient or cationic nature of Md-Pd(111) surfaces enhances the NO dissociation and inhibits oxygen chemisorption ≤400 K under lean-burn conditions.

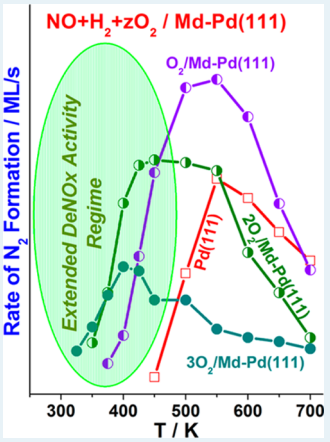

KEYWORDS: *heterogeneous catalysis, nitric oxide, hydrogen, palladium, molecular beam, surface modification, deNO$_x$, lean burn*

1. INTRODUCTION

The selective catalytic reduction of NO$_x$ to nitrogen (deNO$_x$) is a known method for removing this pollutant from stationary as well as mobile sources, such as a three-way catalyst (TWC) converter in automobiles. The aim of TWC used in automobiles is to convert pollutants (NO$_x$, CO, volatile organic compounds (VOCs)) to benign gases, such as N_2, H_2O (and CO_2). Currently employed internal combustion (IC) engines in automobiles work at higher fuel efficiency, that is, at a high air/fuel ratio, than that of their counterparts employed one to two decades ago. Hence, oxidation processes, such as CO oxidation to CO_2 and complete combustion of VOCs, become more favorable; however, in contrast, reduction of NO$_x$ under net oxidizing conditions becomes a serious problem. A predominant challenge to both industrial and academic research is, therefore, the selective reduction of NO$_x$ under predominantly oxidizing or lean-burn conditions. Many deNO$_x$ techniques have been tried so far using different single or multiple reducing components, such as CO, NH_3, urea, hydrocarbons, or H_2. Recently, H_2-selective catalytic reduction (SCR)[1,2] has become of interest for deNO$_x$. The fact is that H_2-SCR is a totally green method because it generates N_2 and H_2O as products. By adopting H_2-SCR, different tricky issues of NH_3-SCR, such as vanadia emission, NH_3 slippage, and air heater fouling, can be easily avoided. The NO$_x$ reduction temperature by H_2 is comparatively lower, and H_2-SCR has technological potential, too, because H_2 is available in many postcombustion methods. H_2 can be generated in diesel engines by auto thermal reforming of diesel.[3] These facts encourage H_2-SCR for on-board deNO$_x$ in IC engines.

The present study focuses on H_2-SCR by palladium under lean-burn conditions. Rh is well-known over Pd for NO reduction to N_2 in first-generation TWC working at a stoichiometric air/fuel ratio (~14.6). Nonetheless, both Rh and Pt form irreversible oxides under net oxidizing conditions, whereas Pd shows more oxygen tolerance. This reason promotes shifting of TWCs from Rh-/Pt-based to Pd-based catalysts.[4] Therefore, the kinetics of the most representative reactions involved on TWCs, such as the NO + H_2 and NO + H_2 + O_2 reactions on Pd-based materials, have been the subject of a wide number of publications from surface science

Received: March 16, 2014
Revised: April 21, 2014
Published: April 23, 2014

   dx.doi.org/10.1021/cs500342a | ACS Catal. 2014, 4, 1801−1811

approaches, performed under ultrahigh vacuum (UHV),[5−9] to more realistic conditions at atmospheric pressures.[10−22]

Direct dissociation probability of NO influences the rate of the NO + H_2 reaction below 373 K. According to Hecker and Bell,[21] and Burch and Watling,[22] an alternative path of NO decomposition, called H_2-assisted NO decomposition, could lead to an increase in the reaction rate; however, the evaluation of single-crystal data concludes that both reactions can be adequately explained by an initial direct dissociation of NO, followed by removal of the fragments by adsorbed reductant. Detailed kinetic and operando spectroscopy work carried out by Granger et al.[18] supports that in the absence of O_2, the dissociation of NO_{ads} species is assisted by chemisorbed H atoms on Pd/Al_2O_3; however, in the presence ofa large excess of O_2, this decomposition is not favorable. In the presence of O_2, hydrogen is easily consumed by oxygen. Oxygen addition increases NO decomposition at relatively low temperatures on $Pd/LaCoO_3$.

The H_2 + O_2 reaction pathway is faster than the NO + O_2 reaction pathway;[10] therefore, oxygen has a detrimental effect on the overall NO + H_2 + O_2 reaction. However, Wen[11] shows that an inhibiting effect of oxygen on NO reduction at 373 K is not significant; rather, it plays a positive role by decreasing the steady-state (SS) concentration of H_2 and, thus, providing more vacant sites for NO. Literature reports also suggest two different mechanistic channels for low- and high-temperature NO reduction processes.[10] Over Pd/TiO_2 catalyst, there were two NO_x conversion maxima observed. IR results showed that the Pd^{2+}−NO, Pd^0−NO, Pd^+−NO, and a bent Pd nitrosyl species existed at 393 K, whereas at 513 K, these bands disappeared, and a new band due to NH_x species on the Lewis acid sites appeared.[12] This phenomenon indicated that the reaction paths were quite different at these two temperatures.

From the above discussion, it is clear that the nature of the active intermediate species and, hence, the reaction mechanism depends on the chemical and electronic nature of the active sites, the support type, and the preparation conditions. In the present manuscript, we address the reaction kinetics of NO reduction by H_2 under net-oxidizing conditions on Pd(111) and a surface that are modified with O atoms in the subsurfaces, called modified Pd(111) (Md-Pd(111) surfaces. The latter is mainly to simulate the calcination conditions carried out on supported Pd-based catalysts employed in the literature.[10−22] Ultraviolet photoelectron spectroscopy (UVPES), and XPS measurements were carried out with ambient pressure photoelectron spectrometer (APPES) in the presence of O_2 at relevant conditions to explore the electronic structure changes under experimental conditions. The present manuscript is part of our efforts in exploring the TWC reactions, such as CO oxidation and NO reduction with different reductants on Pd surfaces.[9,23−32]

2. EXPERIMENTAL SECTION

The isothermal kinetic measurements have been performed in a home-built molecular beam instrument (MBI) using an effusive molecular beam doser. The detailed description of MBI is available in the Supporting Information and in our earlier reports.[23,24] The Pd(111) single crystal (Metal Oxide Ceramics, UK) was cleaned by the standard procedure of Ar^+ sputtering in an oxygen atmosphere (total pressure of 1.5×10^{-6} Torr) at 950 K and subsequent annealing at 1100 K. Temperature-programmed desorption (TPD) spectra were recorded at a constant heating rate of 10 K/s. NO (SG Spectra Gases 99%), H_2(Sigma-Aldrich), and O_2 (Inox Air Products Ltd., 99.999%) were used without any further purification. Control and systematic experiments were measured with a combination of labeled reactants (^{15}NO (99% isotopic purity with 1% ^{14}NO), $^{18}O_2$, (98% pure and 2% of $^{16}O_2$ and $^{18}O-^{16}O$), D_2 (99% isotopic purity and 1% H_2) to measure the contribution from different overlapping mass species, such as $^{15}NH_3$ ($^{15}ND_3$, ND_3, and NH_3) and H_2O (D_2O). Nevertheless, throughout the manuscript, all the reactions are simply mentioned as NO + H_2 + O_2. Whenever a second labeled isotope component was employed, the first two experiments were not taken into account for any calculation or reporting purposes due to facile isotope exchange. Nonetheless, the majority of isotope exchange decreases after the above flushing action, and results obtained thereafter are reported. A total flux (F) of reactants of 0.64 monolayer per second (ML/s) was used in all the experiments reported here unless otherwise specified. The diameter of a Pd(111) single crystal is 8 mm, and 10 mm is the diameter of the molecular beam; 45% of the molecular beam is intercepted at a distance of 5 mm between the molecular beam doser and Pd(111) surface under the experimental conditions reported.[23] Because of high flux conditions on the sample surface, readsorption of gas molecules from the gas phase (after adsorption from direct molecular beam) is small and well within the experimental error limit of 5%.

Isothermal molecular beam experiments were performed on clean Pd(111) and on Md-Pd(111) (O populated in the subsurface) between 325 and 700 K with xNO + $y$$H_2$ + $z$$O_2$ (x:y:z represents the composition of the respective individual components; x = 1, y = 1−4, and z = 0−3). The mass spectrometer signals are calibrated for reactants and products by leaking pure components individually. The contribution from the background to the measurements of the reaction rates was estimated to be within ±5% of that from the direct beam by independent calibration experiments and was not considered for calculations of the SS rates and coverages.[9,23,24] Reaction rates reported are reproducible within 5% error for major products (N_2 and H_2O), and 20% error for minor products (N_2O and NH_3). More details about the MBI experiments and measurement of different kinetic parameters are available in our earlier publications.[9,25,27]

A laboratory version of ambient pressure photoelectron spectroscopy (Lab-APPES)[33] was employed to show the changes in surface characteristics due to O_2 dosing on Pd surfaces. The Lab-APPES unit is equipped with VG Scienta's R3000HP electron energy analyzer (EEA), and it has several advantages that are listed in ref 33. EEA is equipped with three differential pumping stages to maintain a high vacuum under high pressure experimental conditions. Two sets of differential pumping are available in the electrostatic lens regime (ELR), and the third one is available in the analyzer. The distance between the sample surface and the tip of the cone attached to ELR can be decreased up to 100 μm.

The X-ray monochromator (MX650 from VG Scienta) is isolated from the analysis chamber by a thin aluminum window (5 μm). A UV discharge lamp source (UVS40A2, Prevac) with photon flux of 10^{16} photons/s.sr was employed for measuring the valence band (VB). The distance between the sample surface and aperture (of the cone, D = 1.2 mm) attached to the ELR was maintained at 1.4 mm for the experiments reported herewith. Further, a special design of a double front cone pumping arrangement[33] is available in the ELR. The main

dx.doi.org/10.1021/cs500342a | ACS Catal. 2014, 4, 1801−1811

advantage with this design is a fast decrease in pressure with a steep pressure gradient from the aperture to the EEA.

3. RESULTS AND DISCUSSION

3.1. General Considerations. Kinetic runs were carried out for NO + H_2 + O_2/Pd(111) between 400 and 700 K and for NO + H_2 + O_2/Md-Pd(111) between 325 and 700 K. There is no hysteresis observed between temperature ramping from low to high or vice versa. Steady state results reported were reproduced many times within the experimental error limit. Although $^{15}NO_2$ (amu = 47) was also recorded, no measurable intensity was observed, suggesting that there is no NO_2 production under the present experimental conditions. Indeed, no NO_2 was observed in a similar work on Rh(111) and Pd(111) surfaces.[30−36] Many reference experiments were measured with a combination of different isotopes, such as ^{15}NO, $^{18}O_2$, and D_2, to measure the contribution from different overlapping mass numbers, such as $^{15}NH_3$ ($^{15}ND_3$) and H_2O (D_2O). As an example of the results obtained, Figure 1 shows the experimental data for the 1:1:1 beam composition reaction on Pd(111) surface.

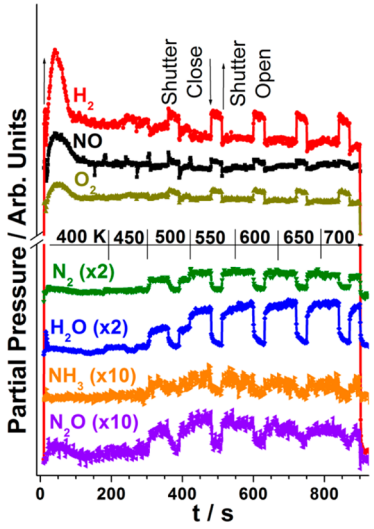

Figure 1. An effusive collimated NO + H_2 + O_2 molecular beam (of 1:1:1 NO + H_2 + O_2 composition in this example) is directed onto a clean Pd(111) surface as the temperature is swept in 50 K steps between 400 and 700 K, and the partial pressures of both reactants (NO, H_2, and O_2) and products (N_2, H_2O, NH_3, and N_2O) are followed as a function of time. The beam is deliberately blocked and unblocked to measure the steady-state rates of different species directly, as they are proportional to the drop (increase) in partial pressure of the products (reactants) from their steady-state values.

Different steps followed in the experiments can be elaborated with reference to Figure 1: (1) The temperature of the crystal is set at 400 K (in this present case). At t = 10 s, the molecular beam of the mixed reactants was turned on, keeping the shutter in a blocked position. The beam cannot react directly to Pd(111) surface. (2) The shutter was unblocked at t = 15 s. The beam can now directly react with Pd(111) kept at 400 K. The system is allowed to evolve until a SS is reached, which generally occurs within 60 s. The time from the unblocking of the beam to the SS reached is termed the transient state (TS). An increase in the reactants' partial pressure at the beginning of reaction was due to a flushing effect of reactants from the inner walls of the UHV chamber, which decreases with time and does not indicate a change in the flux (F) on Pd(111).[24,25,37,38] (3) In the SS, the rate of the reaction was measured by blocking the shutter for 30 s between t = 480 and 510 s at 550 K. An increase (decrease) in the partial pressure of all reactants (products) was observed while blocking the beam in the SS. The above observation and other results presented in this article highlight that the net adsorption is significantly influenced by the reaction conditions. The measured changes in the partial pressure of products allow direct determination of the SS reaction rates, indeed, after calibration with pure components. (4) After the rate measurement through the shutter operation at the first temperature was made, the crystal was heated to measure the SS rate for the next temperature. This procedure was followed to measure the rate at several temperatures up to 700 K in the example shown in Figure 1. (5) Finally, the molecular beam was turned off at t = 920 s (Figure 1). TPD was recorded at a heating rate of 10 K/s after the system again reached UHV.

A systematic study of the NO + H_2 + O_2 reaction kinetics on Pd(111) surfaces was carried out by following the above procedure as a function of temperature and NO/H_2/O_2 composition. A detailed analysis of the kinetic data from NH_3 and N_2O was difficult because of a poor S/N ratio associated with the data. However, at the time of shutter opening or closing, a good change in the partial pressure of all the products (including N_2O and NH_3) demonstrated that a major contribution is due to molecular beam. To understand the NO reduction under net oxidizing conditions, a wide range of temperatures and beam compositions were studied, and the results are described in the following sections.

3.2. Temperature Dependence. Figure 2 displays the kinetic data for time evolution of all products, N_2, H_2O, NH_3, and N_2O, due to reaction of NO + H_2 + O_2 (1:2:1) composition on a Pd(111) surface while ramping the temperature in a stepwise manner between 400 and 700 K, as explained in Figure 1. No significant N_2 production could be observed up to 450 K, but a small but sustainable SS H_2O

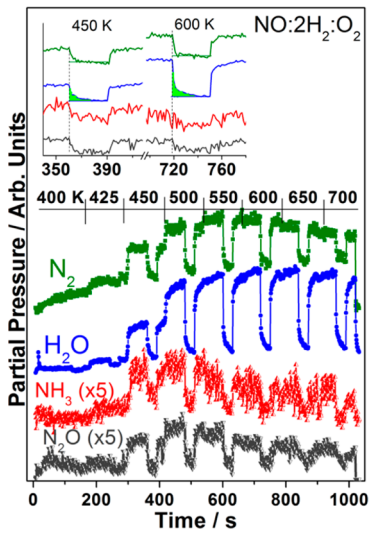

Figure 2. Temperature dependence of the SS rates for the formation of all the products (N_2, H_2O, NH_3, and N_2O) during the conversion of 1:2:1 NO/H_2/O_2 mixtures on Pd(111). Inset shows the decay kinetics of all products and new steady state reached slowly in the case of water formation at 450 and 600 K, suggesting its predominant role in controlling the overall kinetics.

dx.doi.org/10.1021/cs500342a | ACS Catal. 2014, 4, 1801−1811

production occurs from 400 K. At temperatures >450 K, the SS production of N_2 and H_2O increases rapidly with temperature until reaching a reaction maximum between 550 and 600 K. It should be noted that NO decomposition and the onset of NO + CO reaction on clean Pd(111) occurs between 400 and 450 K,[24,25] which is in good agreement with the present results; addition of H_2 and O_2 do not seem to alter the onset of the NO-decomposition temperature. Especially, introduction of oxygen does not significantly change the threshold temperature of NO reduction.

The kinetics observed in the SS for beam oscillation (immediately after shutter closing or opening) for H_2O is quite different from that for N-containing products (Figure 2 inset). Fast changes were observed in the partial pressure of N-containing products on blocking and unblocking the beam, whereas the H_2O pressure changes slowly. A slow change in the partial pressure of water is shown in the fluorescent green shaded area, which is the difference between experimentally observed kinetic decay and if the decay occurs without any delay (or rectangular decay). The main conclusion from this observation is that the diffusion-controlled nature of recombination of H and O atoms to molecular H_2O is likely to be the major rate-determining step (RDS) for the whole process under the conditions of those experiments.

It should be noted that N_2 formation is the RDS with NO + CO + O_2 on Pd(111),[24,30] and the change in reductant from CO to H_2 changed the RDS to water formation. Further, for all N-containing products, the rate decreases at ≥600 K, whereas the water formation rate remains almost the same between 500 and 700 K. This suggests that the decomposition of NO is predominant up to 550 K, and the oxygen supply for water formation is dominated by the NO dissociation. At 550 K and above, molecular oxygen dissociation competes strongly and starts supplying oxygen atoms predominantly for water formation.

It is also to be underscored that water formation remains the RDS at low as well as high temperatures (Figure 2, inset). A simple comparison between the kinetic data shown in Figures 1 and 2, indicating an increase in NH_3 production, occurs with an increase in the H_2 content in the reactant composition. Very similar to the results in Figure 1, a 1:2:1 composition also shows a marginally increasing rate of H_2 and O_2 adsorption at temperatures higher than 550 K, whereas the rate of NO adsorption decreases gradually with increasing temperature (data not shown). This supports the above conclusion of oxygen supply channel changes from predominantly NO dissociation at ≤550 K to O_2 dissociation at ≥550 K. N_2O formation was observed between 450 and 600 K, and it remains a minor product. Much less N_2O formation, suggesting the extent of NO dissociation into N + O, is much higher on Pd(111) surfaces than the interaction of molecular NO with N atoms.

3.3. Beam Composition Dependence. To understand the NO dissociation aspects with increasing O_2 or H_2 content, the NO + H_2 + O_2 reaction was carried out as a function of the reactants' compositions. NO dissociation kinetics were measured by varying one of the reactant concentrations in the beam by fixing the other two as constant. Figure 3 displays the kinetic data of products formation for (a) N_2, (b) H_2O, (c) NH_3, and (d) N_2O on Pd(111) for different beam compositions and in the temperature range of 400−700 K. The NO + H_2 reaction was also measured as a reference, as well as to understand the extent of atomic oxygen contribution to water formation through NO dissociation.

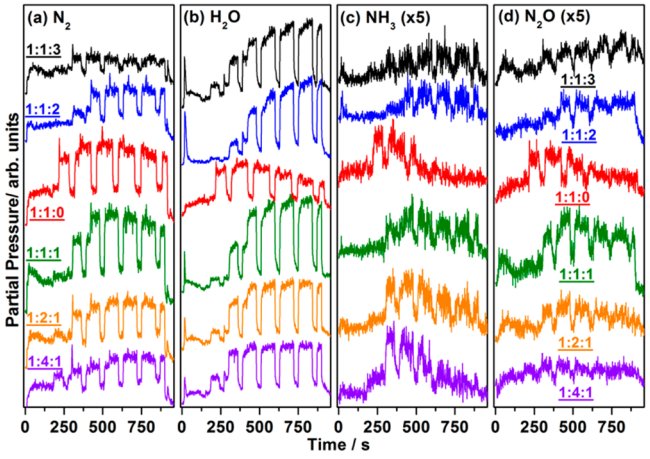

Figure 3. Time evolution of the partial pressure of the products (a) N_2, (b) H_2O, (c) NH_3, and (d) N_2O from the kinetic experiments, such as that described in Figure 1 as a function of temperature and O_2 and H_2 content dependence. ^{15}NO and D_2 were employed, and an initial rise in the partial pressure of amu 30, at the point of turning on the molecular beam, is due to 1% unlabeled NO. The changes in partial pressure of amu 30 under steady state conditions are exclusively due to $^{15}N_2$.

There are a few important observations worth highlighting: (a) The extent of water formation is the lowest, with 1:1:0 composition, and it decreases at >550 K. Oxygen addition to the NO + H_2 mixture increases the rate of H_2O formation and its sustainability at a gradually increasing rate from 550 to 700 K. (b) A large amount of water formation in the TS at 400 K was observed with the oxygen-containing compositions, but it is not sustained in the SS, suggesting the role of adsorption of oxygen atoms derived from molecular oxygen for water formation is limited exclusively to the TS at low temperatures, whereas the NO + H_2 beam does not show any water formation in the TS. (c) A similar rate of N_2 production is evident from the reaction kinetics for 1:1:0 and 1:1:1 compositions, despite a decrease in F_{NO} from 50 to 33.3%. This highlights that a stoichiometric amount of oxygen addition is, indeed, beneficial to NO decomposition. Nonetheless, NO decomposition decreases with an increase in the O_2 content. However, H_2 addition makes the NO decomposition sustainable, even at 700 K, as observed with 1:2:1 and 1:4:1 compositions. (d) N_2 formation (and NO decomposition) is increasingly suppressed at the expense of water formation with a high oxygen content at ≥550 K. (e) Ammonia formation shows a gradual increase with an increase in the amount of H_2 in the mixture of reactants. However, any oxygen addition to the NO + H_2 reactants mixture decreases the ammonia formation, suggesting the predominant H-consumption by O atoms is to form water; this oxygen cleanup facilitates NO dissociation, followed by N + N recombination to form N_2, especially below 550 K. It is also to be noted that, to the best of our knowledge, N_2O adsorption/dissociation on Pd single crystal surfaces has not been reported to date. Our efforts in the past have demonstrated the sticking coefficient of N_2O on Pd(111) is immeasurably small. This aspect, along with other observations, specifically supports the nitrogen forms through N + N recombination rather than through a N_2O intermediate; however, further in situ IR studies are suggested. (f) Although N_2O is a minor product, O_2

dx.doi.org/10.1021/cs500342a | ACS Catal. 2014, 4, 1801−1811

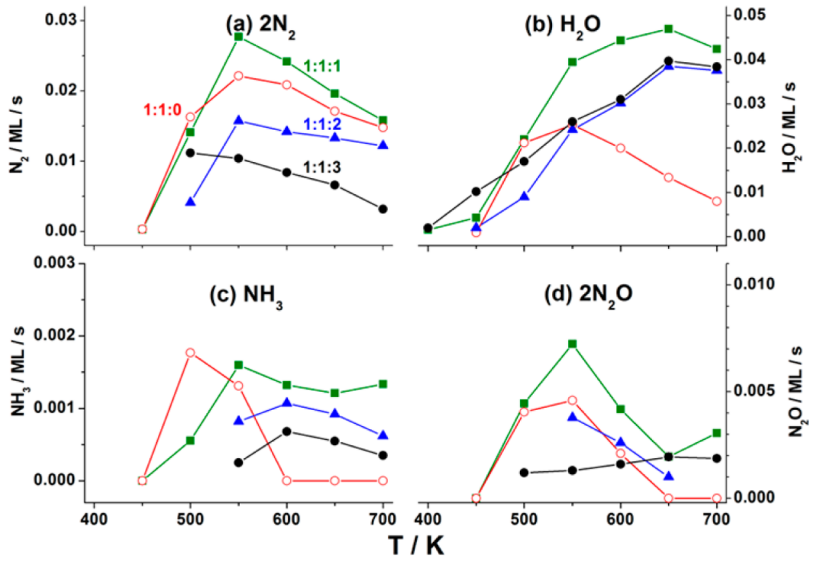

Figure 4. The SS rate measured for all the products from NO + H_2 + O_2 (1:1:z) reaction on Pd(111) surfaces are shown as a function of reaction temperature and O_2 content. (a) $2N_2$, (b) H_2O, (c) NH_3, and (d) $2N_2O$. The rates measured for N_2 and N_2O were multiplied two times because of the consumption of two NO molecules for the production of one molecule of the above products.

addition to a NO + H_2 mixture broadens the N_2O formation regime at high temperatures. Generally, N_2 production was observed from 500 K and above, with the rate maxima observed around 550 K for all of the beam compositions. Notably, H_2 addition enhances N_2 production at higher temperatures and, hence, makes NO dissociation sustainable.

3.4. Effect of Oxygen Addition on NO Dissociation. The steady-state rates measured for various products due to NO + H_2 + zO_2 (z = 0–3) reaction on Pd(111) surfaces between 400 and 700 K are shown in Figure 4. Compositions 1:1:0 and 1:1:1 show similar rate values and a similar trend for N_2 formation. In fact, a marginal increase in rate values with z = 1 indicates the addition of oxygen helps toward more NO decomposition. It is to be noted that F_{NO} decreases from 1:1:0 to 1:1:1, and this fact highlights an effective increase in NO dissociation and, hence, more N_2 production. Simultaneously, the rate of H_2 oxidation to H_2O occurs at a much higher rate with a 1:1:1 composition than with a 1:1:0 composition. For the latter composition, the oxygen supply is exclusively due to NO dissociation, whereas in the case of 1:1:z ($z \geq 1$), O_2 is an additional and main reactant source for the supply of atomic oxygen.

A higher rate of H_2O formation with all O_2-containing compositions than for that of the 1:1:0 composition, especially at ≥550 K, was observed. This result highlights the oxygen cleanup effect by H atoms, which leads to increasingly O-free surfaces with decreasing O_2 content in the reactants' composition. Indeed, this is the reason for the higher rate of N_2 formation with the 1:1:1 composition than that of 1:1:0. However, more O_2 has a detrimental effect on the overall NO dissociation reaction, especially to N_2 production. This can be explained in terms of competitive adsorption of NO and O_2. Despite the availability of oxygen in the 1:1:1 composition, the rate of water (and N_2) formation is the same with both 1:1:1 and 1:1:0 at ≤500 K. This observation confirms the dominance of NO through strong chemisorption, followed by dissociation,[24] over O_2. Nonetheless, an increase (decrease) in the rate of water (N_2) formation at ≥550 K suggests a competitive adsorption by O_2 at the expense of NO and dictates a change in the reaction trend toward more oxidation. Because of the above, surface oxygen coverage (θ_O) increases, and it hinders the NO adsorption as well as decomposition. Addition of O_2 to the 1:1:0 composition initially increases (z = 1) the rate of formation of the minor products; however, with more O_2 (z = 2 or 3), a definite decrease in NH_3 and N_2O was observed. Because of a poor S/N ratio associated with the minor products, as shown in Figure 3, a more meaningful discussion cannot be presented. In conclusion, Pd(111) surfaces show ∼75% selectivity to N_2 and 25% to the total of the other two N-containing products.

From the results shown in Figures 3 and 4, a qualitative trend for the NO and O_2 dominance of the overall NO + H_2 + O_2 reaction is shown below and above 500 K, respectively. Figure 5 shows the quantitative analysis of the rate values of oxygen and NO decomposition by adding 1 mol of oxygen to the 1:1:0 composition. The rate of H_2O formation (R_{H_2O}) values are directly borrowed from Figure 4. The rate of NO decomposition (R_{NO}) was measured from the raw kinetic data as well as calculated from Figure 4 through the following equation (eq 1):

$$R_{NO} = 2R_{N_2} + 2R_{N_2O} + R_{NH_3} \quad (1)$$

It is a fact that the formation of one N_2 molecule requires two N atoms derived from dissociation of two NO molecules. Similarly, formation of one N_2O molecule requires one N atom as well as one NO molecule, which effectively translates into the conversion of two NO molecules. R_{NO} dissociation calculated through the above equation and directly from the experimental results matches within a 10% error limit, and for brevity, the results obtained through the above equation are shown in Figure 5. Further, direct measurement of NO dissociation was not possible below 500 K because of high coverage of different species and, hence, a sluggish rate (Figure 1). The rate of O_2 consumption (R_{O_2}) shown in Figure 5 was calculated by the difference in R_{H_2O} formation between the 1:1:1 and 1:1:0 compositions. There are two important points to be highlighted: (a) A clear demarcation in the results exists

dx.doi.org/10.1021/cs500342a | ACS Catal. 2014, 4, 1801–1811

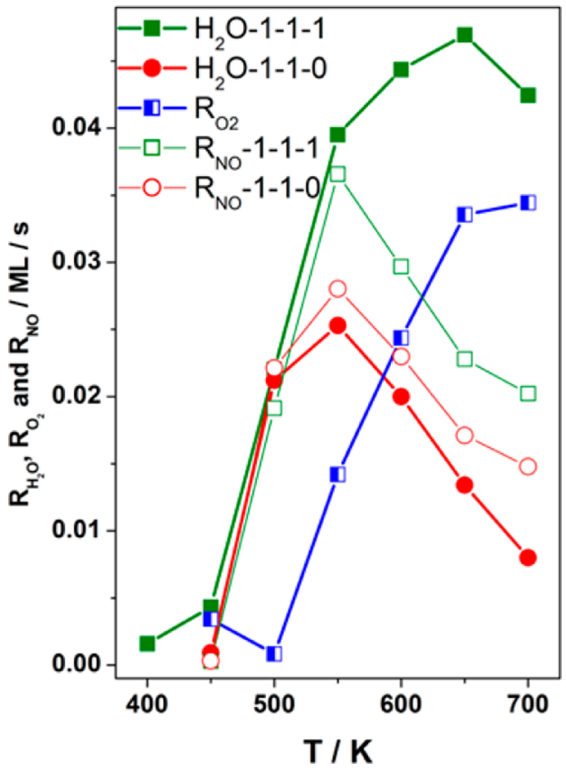

Figure 5. The rate of water formation and NO and O_2 consumption by Pd(111) surfaces is given at different temperatures for the 1:1:0 and 1:1:1 compositions. The rate of NO dissociation matches that of the sum of N-containing products (eq 1) within an error limit of 10%.

between 500 and 550 K, above which R_{O_2} increases with temperature and contributes predominantly toward H_2O formation. Simultaneously, R_{NO} decreases linearly with increasing temperature. However, below 550 K, the overall reaction was dominated by R_{NO}. (b) Despite oxygen addition to the 1:1:0 composition, R_{NO} shows ~30% higher values at ≥550 K with the 1:1:1 composition than with the former and reiterates that some amount of oxygen helps toward increasing R_{NO}. Indeed, hydrogen helps to remove oxygen atoms through water formation.[10]

There are two precautions to be remembered while interpreting the data shown in Figure 5: (a) Because N_2O formation requires consumption of equal amounts of NO molecules and N atoms, the R_{NO} is higher than that of R_{H_2O} for 1:1:0 composition. The amount of molecular NO consumed for N_2O formation does not contribute to water formation, and hence, R_{NO} is higher than R_{H_2O}. (b) R_{H_2O} is expected to be equal to the sum of $R_{NO} + R_{O_2}$ for the 1:1:1 composition (not shown in Figure 5); however, R_{H_2O} is lower than the above sum, especially when the temperature is ≥550 K. This is mainly attributed to the disappearance of some of the O atoms through diffusion into the subsurfaces and possibly into the bulk of the Pd(111) surfaces; this phenomenon is well reported in the literature.[27,39] Indeed, the difference between $R_{NO} + R_{O_2}$ and R_{H_2O} increases at higher temperatures, suggesting the rate of oxygen diffusion into the subsurfaces increases at higher temperatures.

Under practical driving conditions of automobiles, the temperature of the exhaust gases varies widely and influences the performance of TWCC. This would lead to the above such oxygen diffusion into the subsurface and bulk of Pd particles on supported catalysts. In fact, a simple calcination of supported Pd catalysts in air above 550 K would lead to oxygen diffusion and possible partial oxidation of Pd. Many deNO_x researchers adopted such calcination as a pretreatment before NO_x decomposition activity and reported results considerably different from that of the prereduced catalysts.[10−12,16,18] To understand this effect, we embarked on modifying the surface deliberately by exposing the Pd(111) surfaces to high temperatures under an oxygen atmosphere and reevaluated the NO + H_2 + O_2 reactions on the modified surfaces. The results obtained are discussed in the following section.

3.5. Preparation of Modified Pd(111) (Md-Pd(111)) Surfaces. Oxygen diffusion into Pd is a well-known phenomenon.[26,27] There are a significant number of reports available that suggest the formation of different oxide phases (oxide on surface, subsurface; metastable oxides and bulk oxides) due to the interaction of oxygen with Pd at a wide temperature and pressure range.[39−51] The variations in the catalytic activity of Pd in the reactions associated with oxygen have been attributed to the different activities of the different kinds of oxygen species. The role of other moieties, such as C or H, in the Pd subsurface is also worth mentioning.[52] Our group has shown kinetic evidence of the influence of subsurface oxygen on the CO oxidation reaction at high temperatures (600−900 K).[26,27] The effect of subsurface oxygen is remarkable because it changes the electronic nature of the surface as a result of its proximity to the surface, and hence, changes in fundamental adsorption characteristics could occur. A simple vacuum annealing at 1200 K desorbs the subsurface oxygen and brings back the original virgin surface.

We carried out the NO + H_2 + O_2 reaction on Pd(111) with subsurface populated O, and this surface will be represented as modified Pd(111) (Md-Pd(111)). The subsurface oxygen was populated by dosing oxygen at 900 K because it shows maximum subsurface oxygen coverage.[27] CO titration was carried out for each cycle to eliminate the possibility of the presence of any chemisorbed oxygen on the surface. Figure 6 shows the experimental data for $^{18}O_2$ dosing at 900 K, followed by CO titration at 525 K and then reaction of CO + $^{16}O_2$ (3:1) at 500 K. There is a clear uptake of $^{18}O_2$ at 900 K (shaded in pink). After the above oxygen dosage, no CO_2 was observed during CO titration, which rules out the possibility of the presence of any chemisorbed oxygen. During CO + $^{16}O_2$ reaction on the Md-Pd(111) surface, ample oxygen adsorption (shaded in yellow) and product 44 amu (CO_2) formation was observed, whereas the 46 amu ($CO^{18}O$) or 48 amu ($C^{18}O_2$) signal shows no change at all from the beginning of the reaction. This demonstrates that the subsurface oxygen does not diffuse out during the reaction, at least not below 900 K, and its direct participation in the reaction is ruled out; however, during the TPD experiment, subsurface oxygen desorbs between 1050 and 1200 K. Below 1000 K, subsurface oxygen stays within the subsurface and changes the electronic nature of the surface, but without taking part in the reaction. It is to be underscored that under practical driving conditions, the temperature of exhaust gases fluctuates between 473 and 873 K, and it hardly reaches 1000 K; hence, the results presented here have direct relevance to TWCC performance.

3.6. NO + H_2 + O_2 Reactions on Md-Pd(111) Surfaces. The kinetic measurements were made with different NO + H_2 + zO_2 beam compositions (z = 1−3) from 325 to 700 K on

dx.doi.org/10.1021/cs500342a | ACS Catal. 2014, 4, 1801−1811

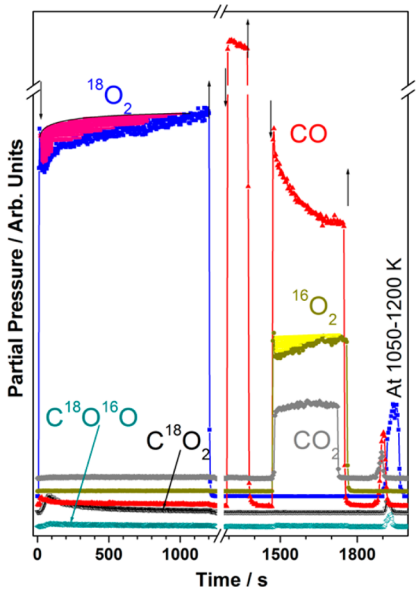

Figure 6. Time evolution of different mass signals (amu's 16, 18, 28, 32, 36, 44, 46, and 48) while dosing $^{18}O_2$ on Pd(111) at 900 K for 20 min, followed by CO titration at 525 K and then CO + $^{16}O_2$ (3:1 ratio) reaction at 500 K. TPD was performed at a heating rate of 10 K/s, after completing the reaction. Remarkably, no increase in 44 ($C^{16}O_2$), 46 ($C^{16}O^{18}O$), and 48 ($C^{18}O_2$) amu during CO titration indicated that the surface does not contain any chemisorbed oxygen. Again, during the CO + $^{16}O_2$ reaction, only the 44 amu signal is evolved without $C^{16}O^{18}O$ or $C^{18}O_2$. This demonstrates that oxygen in the subsurface (^{18}O) does not take part in the reaction. During TPD, subsurface oxygen desorbs between 1050 and 1200 K via molecular O_2 ($^{18}O_2$) and CO_x species with the ^{18}O isotope.

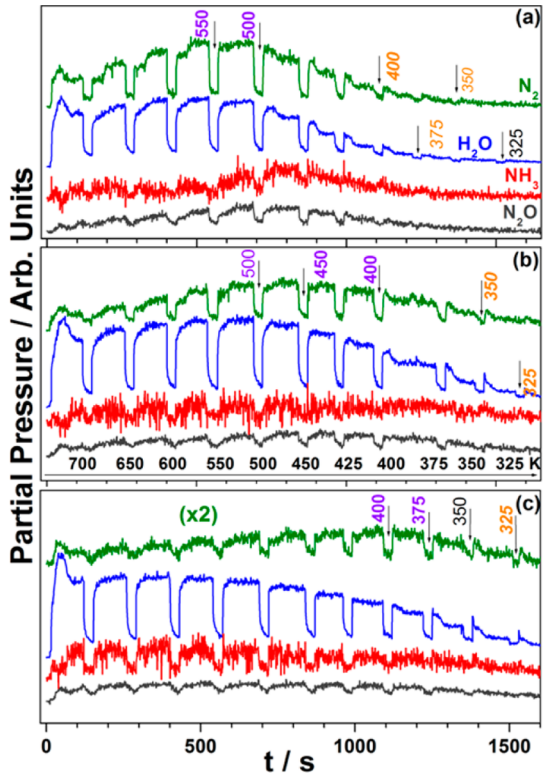

Figure 7. NO + H_2 + O_2 reactions carried out on Md-Pd(111) surfaces from 700 to 325 K with (a) 1:1:1, (b) 1:1:2, and (c) 1:1:3 compositions. Surface modification induces the low temperature activity closer to ambient temperatures. NH_3 and N_2O traces in all panels are multiplied by a factor of 5 and 2, respectively. The rate maximum obtained with N_2 is shown in violet, and introduction of activity at low temperatures is shown in orange. The *y* axis values are maintained the same for all three panels for direct comparison. Reactions were carried from low to high temperature and vice versa, and there was no significant difference or hysteresis observed between them.

Md-Pd(111) surfaces, described in seciton 3.5. Our earlier studies on oxygen diffusion into the subsurfaces of Pd(111) modified the surface characteristics significantly.[9,26,27] This led to an altered catalytic activity toward CO oxidation, and the modified surfaces show CO oxidation activity even at 900 K, whereas virgin Pd(111) shows no significant activity at ≥700 K. We explored a similar aspect toward NO reduction with a NO + H_2 + O_2 mixture as a function of temperature and composition. These measurements were carried out on Md-Pd(111) surfaces (Figure 7), and the results obtained on virgin Pd(111) surfaces (Figure 3) are compared with the above results.

The following points summarize the important findings of the results obtained on Md-Pd(111) surfaces: (1) The 1:1:1 composition on the Md-Pd(111) surfaces shows an extended activity for all products, in comparison with virgin Pd(111) surfaces; N_2 and N_2O products were observed under steady state at least up to 400 K. A very small amount of NH_3 was detected. A tiny, but definite, amount of sustainable water formation was observed, even at 325 K, which is worth noting. The reaction maximum has shifted to 500−550 K on Md-Pd(111) from 550 to 600 K on virgin surfaces (Figures 3 and 4). (2) The 1:1:2 and 1:1:3 compositions on Md-Pd(111) surfaces show the maximum N_2 production activity at 450 and 400 K, respectively, which is much lower than the corresponding results on virgin surfaces (Figure 4). It should also be noted that the high-temperature activity at 700 K is significantly reduced in both cases on Md-Pd(111) surfaces. Further, the N_2 production activity is extended up to 350 and 325 K, with increasing O_2 content in the reactants mixture. Despite decreasing NO-content from 33.3 (1:1:1) to 25 (1:1:2) and 20% (1:1:3), with a concurrent increase in oxygen-content to 60% at 1:1:3 composition, a sustainable NO reduction observed closer to ambient temperature is highly striking. We suggest this aspect may be carefully evaluated with supported Pd catalysts. In fact, Ueda et al.[10] and Lambert et al.[12] reported NO conversion between 10 and 50% at 323 to 373 K, respectively, on Pd/TiO_2 precalcined in air at 773 K, and it compares well with the present results. (3) Water production remains at the maximum between 550 and 650 K for all three 1:1:*z* compositions evaluated. A significant increase in the water production is evident with the 1:1:2 composition. A systematic increase in the low-temperature deNO_x activity is evident from an increasing amount of N_2 and water production. (4) Compared with steady-state values, a significantly higher rate of water production was observed in the TS at 700 K at any given 1:1:*z* composition. A simultaneous increase in N_2 production in the TS underscores a concurrent oxygen cleanup effect occurs, which enhances NO decomposition, even with O_2-rich 1:1:3 composition. This is in stark contrast with the high rate of water formation exclusively in the TS at 400 K than that of the same at steady state on virgin Pd(111) surfaces (Figures 1−3). Although NO content was decreasing, N_2O was detected, and NH_3 production also persisted at a marginal level.

dx.doi.org/10.1021/cs500342a | *ACS Catal.* 2014, 4, 1801−1811

Figure 8 provides a quantitative measure of NO + H_2 + O_2 reaction on Md-Pd(111) surfaces through steady-state rates of

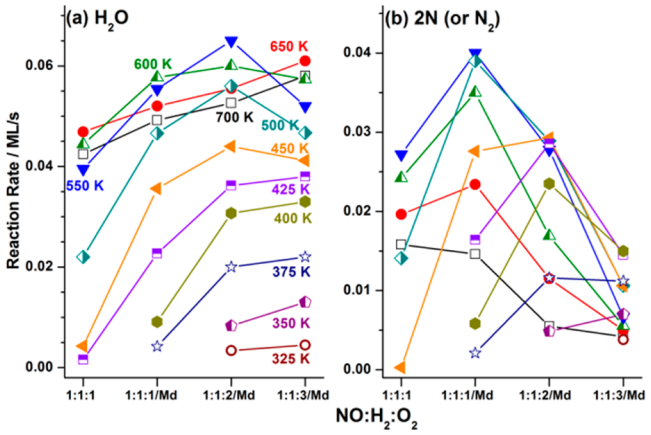

Figure 8. Steady-state rate obtained for (a) H_2O and (b) N_2 from NO + H_2 + O_2 reaction on Md-Pd(111) surfaces carried out with 1:1:z (z = 1−3) compositions between 325 and 700 K. The steady-state rate measured on a virgin Pd(111) surface with a 1:1:1 composition is given for reference. Rate values higher (lower) than 0.005 ML/s were reproduced within a 5% (20%) error limit.

H_2O and N_2 and compared with that of the virgin Pd(111) surfaces. The same results, along with the rate of minor products, are shown in the Supporting Information (Figure S2). Even a glance at the results in Figures 8 and S2 demonstrates a clear broadening of catalytic activity toward ambient temperatures after surface modification. Important points to be highlighted are listed the following: (a) The steady-state NO-reduction activity begins at 450 K on virgin Pd(111) surfaces; however, Md-Pd(111) surfaces exhibit rate values at 450 K that are closer to the rate maximum values. (b) No NO-reduction activity was observed at ≤450 K on Pd(111) virgin surfaces, whereas the rate measurements demonstrate a sustainable NO reduction activity at ≥325 K on Md-Pd(111) with all of the beam compositions, including O_2-rich compositions. (c) The rate of water formation increases linearly for any beam composition from 325 to 600 K on virgin and Md-Pd(111) surfaces. There is a marginal decrease in water production at 650 and 700 K, but they are comparable to the rate observed at 600 K. (d) Essentially, the steady-state rate values observed for N_2 and H_2O with the O_2-rich beam compositions at 325 K is relevant toward cold start deNO$_x$. Even though a large amount of gas phase oxygen is available, the above observation underscores that there may be much less or no O_2 adsorption occurring at low temperature conditions. (e) Although the SS rate of N_2 production decreases gradually at lower temperatures, an increasingly selective N_2 formation is observed on Md-Pd(111) surfaces (Supporting Information Figure S2). The above observation validates NO dissociation closer to room temperatures, without any NH_3 formation and in the presence of excess oxygen (z = 3). NO molecules compete strongly with oxygen for adsorption sites, and the surface may be dominated by an exclusive NO + H_2 reaction. (f) Although the rate maximum lies between 550 and 650 K for H_2O formation on Md-Pd(111) surfaces, the same for N_2 gradually shifts from 550 K toward 400 K with an increasing O_2 content. Selectivity of NH_3, N_2O, and N_2 products is 5 ± 5%, 16 ± 5%, and 76 ± 5%, respectively, at the optimum reaction temperature. Exclusively N_2 was produced at ≤375 K on Md-Pd(111) with O_2-rich composition. Although absolute activity has increased after surface modification, the product selectivity remains largely unchanged.

It is to be noted that there are significant differences as well as similarities observed between the steady-state rates reported in Figure 8 (Supporting Information Figure SI-1) and that of supported Pd-based deNO$_x$ catalysts.[10−13,18] The low-temperature deNO$_x$ onset observed around 325 K is similar in the case of supported catalysts that were precalcined in air[10−13] and the Md-Pd(111) single crystal system. Unlike the two reaction maxima that were observed on supported Pd catalysts,[10−13] only one reaction maximum was observed in our results on Pd(111). This underscores that the role of the support is significant at relatively high temperatures (≥450 K) and likely insignificant at low temperatures.

A careful analysis of the reactants adsorption under the steady state conditions was made, and a representative result is shown in Figure 9. It shows the adsorption of reactants

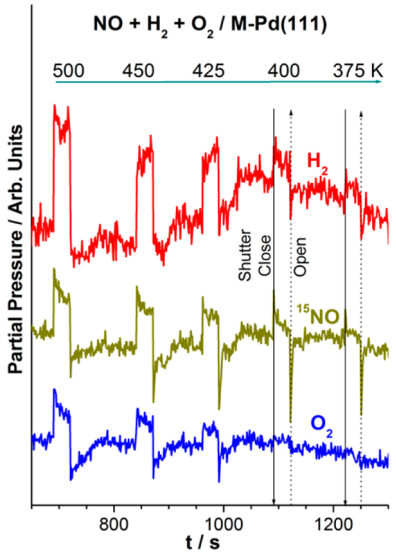

Figure 9. NO, H_2, and O_2 adsorption under steady-state reaction conditions observed for Figure 7a with a 1:1:1 composition between 500 and 375 K. Shutter close and open operations are shown by solid and dotted lines. Although sustainable NO and H_2 adsorption are observed at lower temperatures, simultaneous O_2 adsorption was not observed, suggesting the retardation of oxygen adsorption.

between 500 and 375 K for the results reported in Figure 7a with a 1:1:1 composition. The adsorption of all reactants could be observed between 425 and 500 K through beam oscillation measurements. Nonetheless, below 425 K, no O_2 adsorption could be observed, even though there was O_2 available in the molecular beam; whereas a sustainable NO and H_2 adsorption was observed at temperatures ≤425 K. Indeed, this demonstrates a change in the nature of Md-Pd(111) surfaces, which seems to hinder O_2 adsorption at low temperatures. One-to-one comparison of the reactants uptake at reaction maximum (500 K) and ≤400 K demonstrates a manifestation of exclusive NO + H_2 reaction in the latter (Figure 9).

Indeed, the above results explain in part why the contradicting results are observed for NO + H_2 + O_2 reaction on Pd on different supports, especially between 400 and 300 K.[10−12,18] A small amount of active Pd on any support material should exhibit surface defect sites, and oxygen diffusion into the subsurfaces is a good possibility, which will modify the surface.

dx.doi.org/10.1021/cs500342a | ACS Catal. 2014, 4, 1801−1811

When reactions were measured on modified surfaces, it was expected that they would show significantly different activity from virgin catalysts.

3.7. : Electronic Structure of Md-Pd(111) Surfaces. To explore the nature of surface modification described in the earlier section, APPES measurements were made on exposing Pd surfaces to molecular oxygen at relevant pressures and temperature conditions. Figure 10 shows the representative

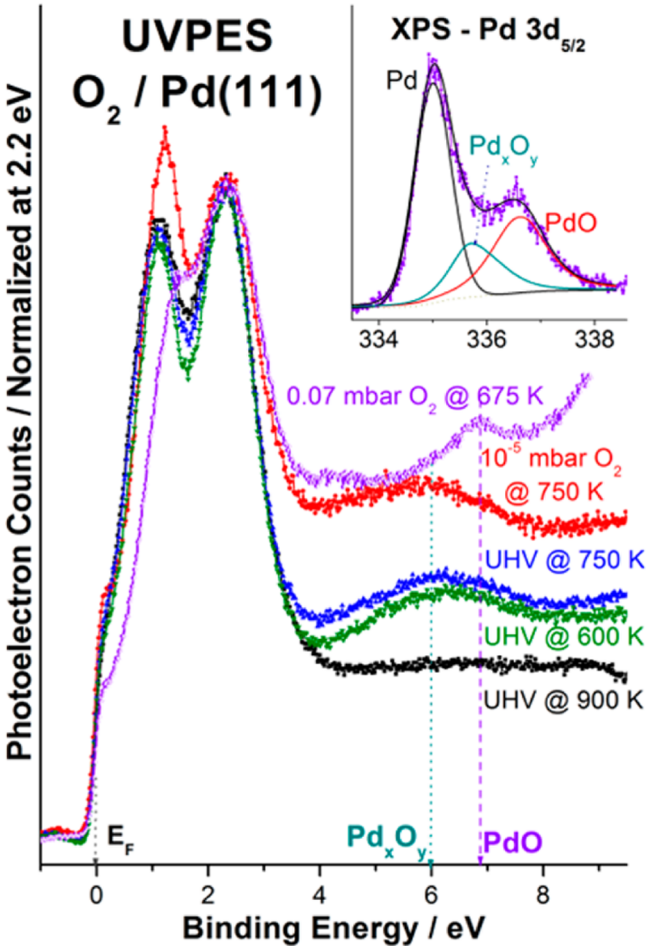

Figure 10. UVPES VB spectra recorded on a Pd(111) surface at different experimental conditions, mentioned on the spectral traces. All the spectra are normalized to the feature at BE = 2.3 eV. Broad and sharp peaks observed at 6 and 6.8 eV are attributed to Pd_xO_y and PdO features, respectively. The inset shows the XPS results recorded at 0.07 mbar O_2 pressure and 673 K for the Pd $3d_{5/2}$ core level, and the contribution from different states are deconvoluted.

APPES results recorded on clean Pd(111) surfaces at UHV (black trace) after surface modification and in the presence of oxygen at 10^{-5} mbar and 900−750 K (red trace) and after evacuation to UHV at different temperatures (blue and green traces). APPES results were also shown at 0.07 mbar O_2 pressure and 675 K (violet trace). It is to be noted that the results presented in Figure 10 are from valence band (VB) photoemission with He I excitation radiation, which is $h\nu$ = 21.2 eV. This is the first time that APPES results have been recorded with low kinetic energy (KE ≤ 16 eV) electrons on Pd surfaces. Our earlier studies with UVPES of systematic Cu oxidation to CuO through Cu_2O with the observation of associated changes in electronic structure at a pressure of 0.3 mbar O_2 at different temperatures is worth mentioning; it demonstrates the capability of Lab-APPES.[33b] More details about the Lab-APPES system are available in our earlier reference.[33]

A clean Pd(111) surface at UHV shows a typical 4d doublet features with a strong Fermi level (E_F) intensity in the VB by UVPES. On introduction of O_2 and modification of Pd(111) surfaces at 1×10^{-5} mbar between 750 and 900 K a new broad feature at 6 eV is shown. An increase in the intensity of the first feature comapred with the second feature in Pd 4d VB is also to be noted. In addition, a small but definite broadening of the VB feature occurs under the above conditions (red trace in Figure 10), highlighting that a considerable change in VB occurs in the presence of oxygen. Even if the surface was exposed to oxygen at 10^{-5} mbar for a longer duration, no significant changes were observed in the VB. After recording the above spectra, oxygen was evacuated, and the VB spectrum was recorded at different temperatures; the results show that the broad feature at 6 eV remains there, but the VB features revert back to that of a clean Pd(111) surface.

The oxygen pressure was increased to 0.07 mbar, and the UVPES was recorded at a temperature of 675 K. There are significantly different changes occurring at high pressures. First and foremost is the observation of a sharp O 2p feature at 6.8 eV. What was observed as a broad feature at 10^{-5} mbar O_2 develops into the above feature, suggesting the precursor nature of the broad feature at 6 eV to the above oxide feature. This also demonstrates the broad feature is oxygen-related, and we attribute this to the oxygen in the immediate subsurfaces, which modify the surface, as shown in Figure 6. The second observation is a significant decrease in the E_F intensity, along with VB's shifting to higher BE (violet trace in Figure 10). The first VB feature at 1.2 eV merged significantly with the second feature. A significant amount of electron density decreases at E_F as well as with the first VB feature and a simultaneous increase in the O 2p feature at 6.8 eV highlights the surface oxide formation under the experimental conditions of 0.07 mbar O_2 and 675 K. Nonetheless, the E_F feature underscores that the oxide formation is restricted to the surface alone.

APPES results recorded with the Pd $3d_{5/2}$ core level at 0.07 mbar O_2 and 675 K is shown in the inset of Figure 10. A distinct Pd $3d_{5/2}$ peak was observed at 336.5 eV and is attributed to PdO. PdO is accompanied by metallic Pd and another feature at 335.0 and 335.7 eV, respectively. The latter feature is attributed to Pd_xO_y or Pd with oxygen in the immediate subsurfaces. In fact, the 2:1 intensity ratio observed between the 336.5 and 335.7 eV features is attributed to Pd with oxygen in the immediate subsurfaces.[9,43,50] It should be noted that UVPES is more surface-sensitive than XPS because of low and high probing depths, respectively, and hence, the buried subsurface feature is easily observed in XPS, even after PdO formation at 0.07 mbar O_2 at 675 K. Upon evacuation to UHV, the VB spectra revert back to the spectra shown for UHV at 600 K.

The above results highlight the presence of O atoms that are diffused into the subsurface layers as Pd_xO_y in the presence of oxygen and after evacuation to UHV. Only a high temperature treatment above 1000 K, removes the subsurface oxygen, as shown in Figure 6. We speculate that this particular species is responsible for near-ambient temperature deNO_x activity. Surface PdO formation occurs exclusively in the presence of oxygen, at least under the conditions studied, and it decomposes on O_2 evacuation. APPES results reported at

dx.doi.org/10.1021/cs500342a | ACS Catal. 2014, 4, 1801−1811

pressures higher than 0.1 mbar make the PdO layers relatively thick.[9,50,51] Nonetheless, that the presence of a reductant, such as H_2, reduces PdO to metallic Pd by consuming oxygen from PdO was aptly demonstrated by exposing the preoxidized Pd-based catalyst (by air calcination at 773 K) and then carrying out NO reduction with NO + H_2 + O_2 at 373 K.[11] Hence, even if PdO layers form as a result of O_2-rich real-world conditions, such as a high partial pressure of oxygen and high temperatures, the same can be reverted back to metallic Pd with oxygen in the subsurfaces when it is exposed to a reductant within the mixture of reactants. In fact, this is the specialty of Pd: to withstand the oxygen-rich conditions and survive under lean burn conditions. However, oxygens in the subsurfaces are intact, unless they are exposed to temperatures higher than 1000 K.

The above observation and discussion demonstrates the applicability of surface modification to shift the catalysis regime toward ambient temperatures. In the above case, Pd surfaces are mildly oxidized as a result of the presence of oxygen in the subsurfaces or in the form of Pd_xO_y. Effectively, this makes the net surface nature cationic ($Pd^{\delta+}$). Elementary processes that occur on the Md-Pd(111) surfaces are shown in a drawing in Figure 11. The cationic character retards any process that

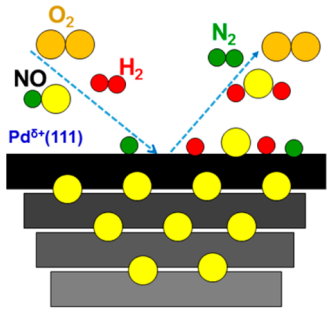

Figure 11. Surface modification is indicated by graded black to gray color with oxygen (yellow circles) in the subsurfaces. Particularly O_2 chemisorption and dissociation (orange solid circle) is hindered or at least minimized, which enhances NO dissociation and $deNO_x$ activity around ambient temperatures.

requires electron donation from the surface; instead, it accelerates electron acceptance from chemisorption. Chemisorption and dissociation of molecular oxygen requires electron donation from the surface, which is retarded at lower temperatures on $Pd^{\delta+}$. In addition, the high electronegativity of oxygen hinders any oxygen dissociation. However, because of the polar nature of NO, chemisorption followed by dissociation occurs readily on $Pd^{\delta+}$. It also should be remembered that molecular NO adsorption occurs below 400 K on clean Pd(111) surfaces[24] as a result of the back-donation of electrons from the surface. On cationic surfaces, the back-donation is likely to be absent, which leads to dissociation of NO molecules and, hence, low-temperature activity. We believe that surface modification with electronegative[26,27] (such as oxygen) or electropositive (such as carbon, hydrogen) atoms[28,52] in the subsurfaces could influence many other reactions, and it is worth exploring.

4. CONCLUSIONS

A possibility of shifting the catalysis regime toward ambient temperatures is demonstrated through surface modification for NO reduction on Pd(111) surfaces. Virgin and modified Pd(111) surfaces were evaluated for NO reduction with technically relevant temperatures and NO + H_2 + O_2 compositions. Compared with virgin surfaces, modified Pd(111) demonstrates not only a 50% increase in $deNO_x$ activity, but also shifts the $deNO_x$ regime toward ambient temperatures. Even though a large amount of oxygen is present in the gas phase, effectively, the NO + H_2 reaction occurs on the modified surfaces, demonstrating the retardation of molecular oxygen adsorption below 400 K. A careful analysis of NO + H_2 and NO + H_2 + O_2 reveals the adsorption and utilization of oxygen from molecular oxygen toward oxidation of hydrogen is very low at temperatures below 500 K. We believe that the cationic character of modified Pd surfaces hinders oxygen adsorption because of a significantly low electron donation capability, which may be probed by other relevant analytical techniques.

An important aspect of the present work to be underscored is the permanence of oxygen atoms diffused into the subsurfaces and, hence, Pd_xO_y. As long as the temperature does not increase above 1000 K, the above feature is stable and exhibits its influence in demonstrating near-ambient temperature $deNO_x$ catalytic activity. Further, surface oxide that forms under oxygen-rich conditions either decomposes or the oxygen in the surface oxide is consumed under fuel-rich or reductive conditions. This exposes the modified surfaces, and hence, the low-temperature activity reverts. In fact, it is highly desirable to explore the modified surfaces for different reduction and oxidation reactions.

■ ASSOCIATED CONTENT

Supporting Information

Complementary plot of Figure 8 is given in Figure SI-1. This material is available free of charge via the Internet at http://pubs.acs.org.

■ AUTHOR INFORMATION

Corresponding Author

*Phone: 0091-20-2590 2043. Fax: 0091-20-2590 2633. E-mail: cs.gopinath@ncl.res.in.

Notes

The authors declare no competing financial interest.

■ ACKNOWLEDGMENTS

K.R. and R.J. thank CSIR, New Delhi for research fellowships. Funding from DST-SERB, New Delhi (SR/S1/PC-16/2012) is gratefully acknowledged.

■ REFERENCES

(1) Savva, P. G.; Costa, C. N. *Catal. Rev. Sci. Eng.* **2011**, *53*, 91−151.
(2) Liu, Z.; Li, J.; Woo, S. I. *Energy Environ. Sci.* **2012**, *5*, 8799−8814.
(3) Deluga, G. A.; Salge, J. R.; Schmidt, L. D.; Verykios, X. E. *Science* **2004**, *303*, 993−997.
(4) Tagliaferri, S.; Koppel, R. A.; Baiker, A. *Stud. Surf. Sci. Catal.* **1998**, *116*, 61−71.
(5) Obuchi, A.; Naito, S.; Onishi, T.; Tamaru, K. *Surf. Sci.* **1982**, *122*, 235−55.
(6) Ma, Y.; Matsushima, T. *J. Phys. Chem. B* **2005**, *109*, 1256−1261.
(7) de Wolf, C. A.; Nieuwenhuys, B. E. *Surf. Sci.* **2000**, *469*, 196−203.
(8) Conrad, H.; Ertl, G.; Kueppers, J.; Latta, E. E. *Surf. Sci.* **1977**, *65*, 245−60.
(9) Roy, K.; Gopinath, C. S. *ChemCatChem.* **2014**, *6*, 531−537.
(10) Ueda, A.; Nakao, T.; Azuma, M.; Kobayashi, T. *Catal. Today* **1998**, *45*, 135−138.
(11) Wen, B. *Fuel* **2002**, *81*, 1841−1846.

(12) Macleod, N.; Cropley, R.; Lambert, R. M. *Catal. Lett.* **2003**, *86*, 69−75.
(13) Macleod, N.; Lambert, R. M. *Catal. Lett.* **2003**, *90*, 111−115.
(14) Lee, Y.-W.; Gulari, E. *Catal. Commun.* **2004**, *5*, 499−503.
(15) Macleod, N.; Cropley, R.; Keel, J. M.; Lambert, R. M. *J. Catal.* **2004**, *221*, 20−31.
(16) Yang, J.-B.; Fu, O.-Z.; Wu, D.-Y.; Wang, S.-D. *Appl. Catal., B* **2004**, *49*, 61−65.
(17) Chiarello, G. L.; Ferri, D.; Grunwaldt, J.-D.; Forni, L.; Baiker, A. *J. Catal.* **2007**, *252*, 137−147.
(18) (a) Dhainaut, F.; Pietrzyk, S.; Granger, P. *Top. Catal.* **2007**, *42/43*, 135−141. (b) Renème, Y.; Dhainaut, F.; Granger, P. *Appl. Catal., B* **2012**, *111−112*, 424−432. (c) Dujardin, C.; Twagirashema, I.; Granger, P. *J. Phys. Chem. C* **2008**, *112*, 17183−17192.
(19) Holmgreen, E. M.; Yung, M. M.; Ozkan, U. S. *J. Mol. Catal. A: Chem.* **2007**, *270*, 101−111.
(20) Leicht, M.; Schott, F. J. P.; Bruns, M.; Kureti, S. *Appl. Catal., B* **2012**, *117−118*, 275−282.
(21) Hecker, W. C.; Bell, A. T. *J. Catal.* **1985**, *92*, 247−59.
(22) Burch, R.; Watling, T. C. *Catal. Lett.* **1996**, *37*, 51−5.
(23) Thirunavukkarasu, K.; Gopinath, C. S. *Catal. Lett.* **2007**, *119*, 50−58.
(24) Thirunavukkarasu, K.; Thirumoorthy, K.; Libuda, J.; Gopinath, C. S. *J. Phys. Chem. B* **2005**, *109*, 13283−90.
(25) Thirunavukkarasu, K.; Thirumoorthy, K.; Libuda, J.; Gopinath, C. S. *J. Phys. Chem. B* **2005**, *109*, 13272−13282.
(26) Gopinath, C. S.; Thirunavukkarasu, K.; Nagarajan, S. *Chem.—Asian J.* **2009**, *4*, 74−80.
(27) Nagarajan, S.; Thirunavukkarasu, K.; Gopinath, C. S. *J. Phys. Chem. C* **2009**, *113*, 7385−7397.
(28) Nagarajan, S.; Thirunavukkarasu, K.; Gopinath, C. S.; Counsell, J.; Gilbert, L.; Bowker, M. *J. Phys. Chem. C* **2009**, *113*, 9814−9819.
(29) Nagarajan, S.; Gopinath, C. S. *J. Indian Inst. Sci.* **2010**, *90*, 245−260.
(30) Nagarajan, S.; Thirunavukkarasu, K.; Gopinath, C. S. *J. Phys. Chem. C* **2011**, *115*, 21299−21310.
(31) Nagarajan, S.; Thirunavukkarasu, K.; Gopinath, C. S.; Prasad, S. D. *J. Phys. Chem. C* **2011**, *115*, 15487−15495.
(32) Bowker, M.; Counsell, J.; El-Abiary, K.; Gilber, L.; Morgan, C.; Nagarajan, S.; Gopinath, C. S. *J. Phys. Chem. C* **2010**, *114*, 5060−5067.
(33) (a) Roy, K.; Vinod, C. P.; Gopinath, C. S. *J. Phys. Chem. C* **2013**, *117*, 4717−4726. (b) Roy, K.; Gopinath, C. S. *Anal. Chem.* **2014**, *86*, 3683−3687.
(34) (a) Bustos, V.; Gopinath, C. S.; Unac, R.; Zaera, F. *J. Chem. Phys.* **2001**, *114*, 10927−10931. (b) Zaera, F.; Gopinath, C. S. *J. Mol. Catal. A: Chem.* **2001**, *167*, 23−31.
(35) Zaera, F.; Wehner, S.; Gopinath, C. S.; Sales, J. L.; Gargiulo, V.; Zgrablich, G. *J. Phys. Chem. B* **2001**, *105*, 7771−7774.
(36) (a) Gopinath, C. S.; Zaera, F. *J. Catal.* **2001**, *200*, 270−287. (b) Zaera, F.; Gopinath, C. S. *J. Chem. Phys.* **2002**, *116*, 1128−1136.
(37) (a) Gopinath, C. S.; Zaera, F. *J. Phys. Chem. B* **2000**, *104*, 3194−3203. (b) Gopinath, C. S.; Zaera, F. *J. Catal.* **1999**, *186*, 387−404.
(38) Johanek, V.; Schauermann, S.; Laurin, M.; Gopinath, C. S.; Libuda, J.; Freund, H. J. *J. Phys. Chem. B* **2004**, *108*, 14244−14254.
(39) Klotzer, B.; Hayek, K.; Konvicka, C.; Lundgren, E.; Varga, P. *Surf. Sci.* **2001**, *482−485*, 237−242.
(40) Lee, A. F.; Naughton, J. N.; Liu, Z.; Wilson, K. *ACS Catal.* **2012**, *2*, 2235−2241.
(41) Zemlyanov, D.; Kloetzer, B.; Gabasch, H.; Smeltz, A.; Ribeiro, F. H.; Zafeiratos, S.; Teschner, D.; Schnoerch, P.; Vass, E.; Haevecker, M.; Knop-Gericke, A.; Schloegl, R. *Top. Catal.* **2013**, *56*, 885−895.
(42) Gabasch, H.; Knop-Gericke, A.; Schloegl, R.; Borasio, M.; Weilach, C.; Rupprechter, G.; Penner, S.; Jenewein, B.; Hayek, K.; Kloetzer, B. *Phys. Chem. Chem. Phys.* **2007**, *9*, 533−540.
(43) Gabasch, H.; Unterberger, W.; Hayek, K.; Kloetzer, B.; Kleimenov, E.; Teschner, D.; Zafeiratos, S.; Haevecker, M.; Knop-Gericke, A.; Schloegl, R.; Han, J.; Ribeiro, F. H.; Aszalos-Kiss, B.; Curtin, T.; Zemlyanov, D. *Surf. Sci.* **2006**, *600*, 2980−2989.
(44) Leisenberger, F. P.; Koller, G.; Sock, M.; Surnev, S.; Ramsey, M. G.; Netzer, F. P.; Klotzer, B.; Hayek, K. *Surf. Sci.* **2000**, *445*, 380−393.
(45) Rose, M. K.; Borg, A.; Dunphy, J. C.; Mitsui, T.; Ogletree, D. F.; Salmeron, M. *Surf. Sci.* **2004**, *561*, 69−78.
(46) Titkov, A. I.; Salanov, A. N.; Koscheev, S. V.; Boronin, A. I. *React. Kinet. Catal. Lett.* **2005**, *86*, 371−379.
(47) Han, J.; Zemlyanov, D. Y.; Ribeiro, F. H. *Surf. Sci.* **2006**, *600*, 2730−2744.
(48) Han, J.; Zemlyanov, D. Y.; Ribeiro, F. H. *Surf. Sci.* **2006**, *600*, 2752−2761.
(49) Kan, H. H.; Shumbera, R. B.; Weaver, J. F. *Surf. Sci.* **2008**, *602*, 1337−1346.
(50) Ketteler, G.; Ogletree, D. F.; Bluhm, H.; Liu, H.; Hebenstreit, E. L. D.; Salmeron, M. *J. Am. Chem. Soc.* **2005**, *127*, 18269−18273.
(51) Teschner, D.; Pestryakov, A.; Kleimenov, E.; Haevecker, M.; Bluhm, H.; Sauer, H.; Knop-Gericke, A.; Schloegl, R. *J. Catal.* **2005**, *230*, 186−194.
(52) Armbruester, M.; Behrens, M.; Cinquini, F.; Foettinger, K.; Grin, Y.; Haghofer, A.; Kloetzer, B.; Knop-Gericke, A.; Lorenz, H.; Ota, A.; Penner, S.; Prinz, J.; Rameshan, C.; Revay, Z.; Rosenthal, D.; Rupprechter, G.; Sautet, P.; Schlögl, R.; Shao, L.; Szentmiklosi, L.; Teschner, D.; Torres, D.; Wagner, R.; Widmer, R.; Wowsnick, G. *ChemCatChem.* **2012**, *4*, 1048−1063.